https://doi.org/10.33472/AFJBS.6.5.2024. 8418-8438

AfricanJournalofBiological Sciences

Optimization of meloxicam-phospholipid complex employing QbD based Box-Behnekn design for enhanced formulation efficacy

Authors: Vaibhav Bhadange[1,2], Supriya Jogdand[3], Ankita, Kawtikwar[1], Pravin Kawtikwar[1]*

Affiliation

1. SudhakarraoNaik Institute of Pharmacy, Nagpur Road, SH-183, District Yavatmal, Pusad, Maharashtra-445215
2. Amity Institute of Pharmacy, Amity University Maharashtra, Mumbai-Pune Expressway Bhatan, Panvel, Mumbai-410206
3. Vidyabharati College of Pharmacy, C.K. Naidu Marg, Camp, Amravati-444602

***Corresponding author**

Dr.Pravin Kawtikwar
SudhakarraoNaik Institute of Pharmacy, Nagpur Road, SH-183, District Yavatmal
Pusad, Maharashtra-445215, Email: pskawtikwar@rediffmail.com

Article History
Volume 6, Issue 5, 2024
Received: 22 May 2024
Accepted: 29 May 2024
doi:*10.33472/AFJBS.6.5.2024. 8418-8438*

Abstract

The phospholipids complexation technique is the best solubility enhancement technology, and as a result, many authors have successfully used it to increase the solubility, permeability, and oral bioavailability of numerous drug molecules. The drug belongs to BCS calss II which having poor solubility and higher permeability could have been limited clinical use. Hence the strategy to alter the biopharmaceutical properties should be employed. In this study the Mlx-phospholipid (Mlx-PL) complex was prepared for enhancement of solubility and efficacy of meloxicam which is an NSAID having proven anticancer activity. The Mlx-PL complex was synthesized by solvent evaporation method and quality attributes were optimized by QbD based Box-Behnekn design of experiment. The optimized formulation was evaluated for physicochemical properties and functional patrameters like entrapment efficiency and drug release study. The cytotoxicity study was also carried out in humane adenocarcinoma breast (MCF-7) cell line. The prepared complex was demonstrated form dynamic light scattering which shows particle size distribution of about 122.4 nm and zeta potential about −35.8 mV. The thermal analysis and FTIR study revealed the compatibility of drug with the excipients. It also showed the successful formation of Mlx-PL complex with improved solubility when evaluated for apparent solubility in various organic solvents and in water. The Mlx-PL complex entrapped about 91.77% drug encapsulation and releases the 94.85±3.0% drug after the end of 72 h when demonstrated for in vitro drug release study. The in vitro cytotoxicity study showed enhanced efficacy of Mlx-PL complex than the pure Mlx suspension. Hence the overall results of this study proved the excellent potential of phospholipid complex for solubility enhancement and improved efficacy of the anticancer drugs which belongs to BCS class II.

Keywords: Meloxicam; solubility enhancement; Quality by Design; phospholipid complex; bioavailability

1. Introduction

A non-steroidal anti-inflammatory drug (NSAID) such as meloxicam (Mlx) preferentially inhibits the inducible isoform of the COX-2 enzyme. The prostaglandin production enzyme COX-2 serves as a catalyst, and it has been extensively researched for its potential role in the emergence of cancer. It affects angiogenesis, apoptosis, and is also implicated in the synthesis of carcinogens [1]. Meloxicam (Mlx) is belongs to the BCS class II and showed proven anticancer activity [2]. Mlxwidely use in inflammation and administered orally in the form of conventional tablet dosage form. But the use of Mlx clinically in cancer therapy had some limitations due to the poor aqueous solubility. Although the higher permeability may be the advantageous after the solubility enhancement of the Mlx. There were very limited literature available on the use of Mlx in cancer treatment. Hence there is need to explore the potential of Mlx as a cancer therapeutics.And there is requirement of designing of work to improve the solubility of the Mlx.

The best solubility enhancement approach is the phospholipids complexation method, and various authors have used it to successfully increase the solubility, permeability, and oral bioavailability of numerous extracts and plant bioactives. This comprises, among others, the herbal extracts from*Bacopamonnieri* extract [3], *Centellaasiatica* extract [4], apigenin [5], umbelliferone [6], and daidzein [7]. Phospholipids complexation technology combines phospholipids with extracts and/or medications to create molecular aggregates that are compatible with lipids. Due to a variety of advantages, easier methods of preparation, ability for higher drug loading capacity, improved stability, controlled release of drug, improved efficacy, minimization of side effects, and stomach protection from luminal enzymes, this approach has piqued the interest of researchers. The main element of this system, Phospholipon® 90H, behaves similarly to plasma membrane phospholipids. Any lipophilic drug's polar components can be successfully interacted with by the phosphate (+) charged Phospholipon® 90H to produce an amphiphilic molecule. This amphiphilic compound can further enhance the therapeutic efficacy of extract molecules by facilitating their movement across lipid-rich biomembranes.

This beneficial interaction results in free rotation ofits fatty acid chain. It causes the extracts' particles to become amorphous and wet at the molecular level through particle dispersion into the phospholipids matrix, which increases their solubility and rate of dissolution. Due to its potential advantages, including non-stickiness, high biocompatibility, biodegradability, enzyme activity, and minimal toxicity, it is also a more alluring carrier for the creation of phospholipids complex[5,8,9]. Additionally, the solvent evaporation approach for making phospholipid complexes can produce amphiphilic complexes, which can more effectively

entrap drugs. This makes it easier for complex loaded compound to go from the water-soluble site of the cell membrane to the lipid-soluble area for demonstrating high therapeutic efficacy [10].Based on the beneficial solubility improvement effects of phospholipids complex system, in the present investigation the attempt was carried out to enhance the solubility of meloxicam, which corresponds to BCS class II.Hence the aim of study was to develop, optimize and evaluate the meloxicam-phospholipid complex for solubility enhancement. The formula was optimized by employing QbD base BBD and then evaluated for physicochemical properties along with functional characteristics. The cytotoxicity was determined in MCF-7 cell lines.

2. Material and methods

2.1 Material

Ramdev Chemicals Pvt. Ltd., Thane, (Maharashtra), India provided meloxicam (Mlx) as a gift. We bought Phospholipon® 90H from Lipoid GmbH in Ludwigshafen, Germany. n-hexane, DMSO, 1,4-dioxane, methanol, ethanol, and chloroform were procured from Fischer Scientific Pvt. Ltd.All reagents, solvents and chemicals used were of analytical grade.

2.2 Preparation of Mlx-PL Complex

Meloxicam-phospholipid (Mlx-PL) complex were prepared by modification of previously reported solvent evaporation technique [11].The formula was optimised using the Box Behnken Design of Experiment.Briefly, the weighed amount of Mlx (~100 mg) dissolved in mixture of DMSO (1.5 mL) and chloroform (2 mL). To this solution about 100-300 mg Phospholipon® 90Hwas added and dissolved by further addition of 1,4-dioxane.The whole mixture was then reflux at 60 to 70°C for 4-6 h on water bath. After heating in a water bath, the reaction mixture was allowed to condense. A small amount of n-hexane—about 3–4 mL—was added to this saturated mixture.The resultant mixture was kept in refrigerator overnight.On next day the mixture wasallowed to precipitate with distilled water. The supernatant was decanted and dried overnight at room temperature. FurtherMlx-PL complex with %yield about 94% was stored in airtight glass vial at room temperaturefor analysis.

2.3 Design ofExperiment

To optimise the formulation and/or processing parameters, Box-Behnken design approach was used for designing the experiments [12]. This approach was used to examine the overall impact of independent variables on dependent variables, including phospholipid

(X_1, mg), temperature (X_2, °C), and time (X_3, h). Three distinct parameters were taken into account to optimise the formulation and processing attributes at three levels: low (-1), middle (0), and high (+1) (see Table 1) [13].The concentration of phospholipids (X_1, mg) was used as a formulation attribute, while temperature (X_2, °C), and time (X_3, h) were used as processing characteristics, and there were a total of 17 combinations that can be made utilising all the independent factors.All 17 combinations discovered during experiment design, as shown in Table 2, were used for the experimental trials. To evaluate the reactions, the mathematical model including coefficient effects, interactions, and polynomial terms was analysed [13, 14] utilising the given formula in equation 1:

$Y = b_0 + b_1X_1 + b_2X_2 + b_3X_3 + b_{12}X_1X_2 + b_{13}X_1X_3 + b_{23}X_2X_3 + b\ X\ 2 + b\ X\ 2 + b\ X\ 2$ Eq.1

Y =response, X_1= Conc. of phospholipid in mg, X_2=reaction temperaturein °Cand X_3=time in hour.

Table 1: Independent and dependent quality attributesat three level Quality by Design

Variables	Levels		
	-1	0	+1
		Real Value	
Independent			
Conc. of Phospholipid (X_1, mg)	100	200	300
Temperature (X_2, °C)	60	65	70
Time (X_3, h)	4	5	6
Dependent			
% Yield (Y, %)			

2.4 Apparent solubility analysis

The concentration of the substance in the solvent at super-saturation equilibrium is represented by the apparent solubility. Using a modified approach previously described by Saoji and colleagues, we looked at the apparent solubility of Mlx and the Mlx-PL complex in this study [4,11]. In order to obtain dispersion, 5 mg of Mlx and Mlx-PL-complex were combined with 5 mL of pure water and n- hexane. This was centrifuged for 30 minutes at 4000 RPM after being agitated constantly at 25℃ for 24 h. Centrifugation resulted in thecollection of the supernatant. Then, using a membrane filter (0.45), insoluble particulate matter was separated from the collected supernatant. Following filtration, the filtrate was diluted with DMSO, and the concentration of Mlx was determined at 362 nm using a UV-spectrophotometric technique.

2.5. P**hysicochemical characterization**

2.5.1 Particle size, size distribution and zeta potential measurement

The prepared Mlx-PL complex's particle size and size distribution were examined using the DLS-based system [7]. In a nutshell, de-ionized water containing cuvetes was used to transfer and distribute 5 mg of dried Mlx-PL complex. This was put into the Malvern Zetasizer instrument chamber, and measurements were made at 25 °C. The zeta potential of the Mlx-PL complex was determined using a nano sizing device (Malvern Zetasizer) between the zeta potential ranges of -200 to +200 mV [15].

2.5.2 Thermal analysis

The polymorphic condition of the Mlx, Phospholipon® 90H, PM, and the created Mlx-PL complex was examined using DSC. As a purge gas, dried nitrogen gas at an 80 mL/min flow rate was employed. In a nutshell, an aluminium pan containing around 5 mg of powdered sample was stored in the instrument chamber. A single heating cycle that gradually raised the temperature from 40 °C to 400 °C at a rate of 10 °C min^{-1}. TA software that came with the device was used to analyse the collected peaks [15, 16].

2.5.3 FTIR spectroscopy

By acquiring the IR spectra of Mlx, Phospholipon® 90H, and their PM, the interaction between the elements required to produce the Mlx-PL complex was examined. The FTIR spectra of the Mlx-PL complex was also recorded using FTIR spectrophotometer (FTIR-8300). In a nutshell, 200 mg of potassium bromide (KBR) was uniformly mixed with 2 mg of test sample before being further compressed under 10 ton/nm^2 pressure to create circular discs. For the purpose of removing any potential influence from residual moisture, the samples were first dried for two hours in a hot air oven at 50 °C. Each study consists of 45 scans with a 4 cm^{-1} resolution in the 4000 to 400 cm^{-1} wavelength range [17].

2.5.4 Powder X-ray diffractometry (P-XRD)

Employing an X-ray diffractometer (Model: D8 ADVANCE, Bruker AXS, Inc., Madison, WI, USA) in conjunction with an optical Bragg-Brentano geometry (/2) configuration to obtained their X-ray diffraction pattern. The polymorphic condition of the Mlx, Phospholipon® 90H, PM, and the created Mlx-PL complex was examined. In a nutshell, the samples that would be subjected to analysis were exposed to monochromatic CuK radiation (λ= 1.5406) operating at 30 mV and 10 mA, respectively. With a step-angle of 0.04° 2 in every 5 seconds, the diffraction angle was raised from 3° to 60°, 2. The samples had an angular rotation of 360° [18].

2.5.5 SEM analysis

Examining the morphological structural characteristics has been done using scanning electron microscopy (SEM). A small amount of Mlx-PL complex was placed on a specimen tab and transferred to a slide. After applying palladium coater, the sample was ready for SEM microscopic analysis. Then, SEM pictures were captured using a Carl Zeiss lens and a scanning electron microscope (JEOL JSM-6701F Field Emission) [19].

2.6 Entrapment efficiency

As described in a previously published study [18], the free drug from the Mlx-PL complex was separated by centrifugation technique in order to assess the degree of entrapment. A micropipette was used to pipette out the supernatant, which was then diluted and used for analysis. At 362 nm, the samples were examined.

The calculation of %EE was done using following equation 2.

$$\% EE = \frac{(Total\ Drug - Unentrapped\ \ Drug)}{Total\ Drug} \times 100 \qquad \text{Eq2}$$

2.7 In vitro drug release

The *in vitro* drug release investigation was performed using the methodology outlined in earlier works of literature [20]. Briefly, the aqueous suspension of Mlx-PL complex was introduced into the Franz diffusion cell (donor compartment). The phosphate buffer saline (pH of 7.4) was poured into the receptor compartment. Between the donor and receptor compartments of the diffusion cell, the dialysis membrane was installed. The aqueous solution of Mlx-PL complex containing about 10 mg of drug in equivalent amount of Mlx-PL complex powder (~20 mg) was introduced in donor compartment. At predefined intervals, samples were taken from the side arm, and the medium was then supplied with an equivalent volume of pH 7.4 PBS. The collected samples were analysed on UV-spectrophotometer at 362 nm.

2.8 In vitro cytotoxicity study

The MCF-7 cell line was used for a 72-hour cell toxicity research of Mlx and Mlx-PL complex, and the IC50 was determined using the MTT test. Using the MTT assay, Mlx and Mlx-PL complex were tested for in vitro cytotoxicity in MCF-7 cells for 72 h [21, 22]. To illustrate cytotoxicity, a 96-well plate with 10,000 cells per well was employed. With phenol red-free DMEM, the Mlx and Mlx-PL complex were diluted to various quantities (2, 8, 12, 20, and 40 g/mL). About 200 µL of sample solutions were added to the media, and the

mixture was then incubated at 37 °C in a CO_2 incubator for 72 h. Following incubation, the medium was changed for fresh media, 50 µL of MTT reagent (1 mg/mL in PBS) was added to each well, and the incubator was maintained at 37 °C for 3 hours. Following the removal of the medium, 160 µL of DMSO was used to solubilize the intracellular formazan. The absorbance at 570 nm was measured using SpectraMaxM2 with SoftMax Pro (Molecular Devices Corporation Sunnyvale, CA, USA). The media gave the cells treatment.

2.9 Statistical analysis

The physicochemical analysis and *in vitro* studies data are shown as mean standard deviation. The statistical analysis made use of one-way analysis of variance (ANOVA), Dunnett's, and Student's t-tests. P-values of 0.05 were deemed statistically significant.

3. Results and discussion

3.1 Formula optimization

Quality by Design based BBD was used for formula optimization of Mlx-PL complex. The influence of the various independent variables on the response was studied [16].This study looked at how the independent variables X_1 (Phospholipid Concentration, mg), X_2 (Reaction Temperature, °C), and X_3 (Reaction Time, min) affected the dependent variable Y (% Yield, w/w) of the Mlx-PL complex. The results of the investigation utilising BBD indicate that all three factors have a substantial impact on the yield of the Mlx-PL complex, as shown in Table 2. The seventeen different batches showed % yield in the range of 63.59 to 95.23%w/w.

Study was conducted on the effects of reaction temperature and phospholipid content on yield. From the contour plot and 3D surface plot, the conclusion was reached. The figure 1A and 1B illustrated the effect of $X_1$and X_2 onresponse Yof theMlx-PL complex.The graphs represents the positive influence of phospholipid concentration on % yield. The percentage yield was rise along with the increase in phospholipid concentration up to a point, but then started to fall. Reaction temperature (X_2) had similar impacts on the percent yield of the Mlx-PL complex.The beneficial influence on response (Y) is depicted in Figure 1C and 1D as a contour and 3D surface plot of X_1 and X_3. These figures show that the yield percentage increases progressive with an increase in response time, but that it increases with an increase in phospholipid concentration only up to a point before declining at the very end.

It was also investigated how reaction temperature (X_2) and reaction duration (X_3) affected the response (Y) (see Figure 1E and 1F). Here, X_2 has a favourable effect on the yield of the Mlx-PL complex because it causes the yield to grow as the temperature and time of the reaction increase.

The researched parameters X_1, X_2, and X_3 had a significant impact on the % Yield, which is also demonstrated in equation (2), according to the contour and 3D surface plots. Up to a certain point, increasing the levels of X_1, X_2, and X_3 from -1 to +1 was beneficial for better percent yield of Mlx-PL complex. The optimal level of phospholipid, temperature at which to react, and reaction duration were 200 mg, 65°C, and 5 h, respectively, based on the quadratic model and anticipated regression values. Polynomial equation shown below reflects the overall observations as well;

$$\%Yield = +94.83+10.26A+3.04B+1.74C+0.0100AB-1.11AC+0.9625BC-11.49A^2-7.11B^2 -4.52C^2 \quad \text{Eq. 3}$$

Real factors are used in this polynomial equation 2 to show how they affect the result Y. The positive sign in the equation above indicates a factor's favourable impact on the answer, whereas the negative sign indicates a factor's unfavourable impact. All of the coefficients in the equation were shown to be statistically significant (p 0.05) by the outcomes of the model fitting and the ANOVA.

Given the Model F-value of 57.87, the model is most likely significant. Only 0.01% of the time may noise be the cause of an F-value this high. When the P-value is less 0.0500, model terms are deemed significant. The relevant model terms in this case were A, B, C, and A2, B, and C2. If the value is higher than 0.1000, model terms are not significant. If your model has many extraneous terms (apart from those required to maintain hierarchy), model reduction may improve it. The significance of the lack of fit is indicated by the lack of fit F-value of 12.21. A significant Lack of Fit F-value can only be explained by noise in 1.76% of cases. We want the model to fit, so a significant lack of fit is negative.

Table 2: Seventeen separate batches with every possible combination were created using the Box-Behnken technique based on QbD.

Run	Batch	Independent Variables			Dependent Variables
		X_1	X_2	X_3	Y_1
1	FF1	300	65	6	91.82
2	FF2	300	60	5	83.36
3	FF3	300	65	4	87.74
4	FF4	300	70	5	88.22
5	FF5	200	70	6	88.15
6	FF6	200	60	6	78.91
7	FF7	200	60	4	80.17

8	FF8	200	65	5	95.23
9	FF9	200	65	5	94.11
10	FF10	200	65	5	94.2
1	FF11	200	70	4	85.56
12	FF12	200	65	5	96
13	FF13	200	65	5	94.6
14	FF14	100	60	5	64.25
15	FF15	100	65	4	63.59
16	FF16	100	65	6	72.12
17	FF17	100	70	5	69.07

3.2 Validation of model

The % bias for the model predicted value and the actual value should be less than 3%. Then only the model fitted and validated. In this study, for BBD the % bias was found to be less than 3% hence the model was fitted and validated.

Table 3: Model- Predicted and observed values of % Yield

Complex	**Predicted % Yield (w/w)**	**Observed % Yield (w/w)**	**% Bias**
Mlx-PL complex	94.83	96	1.2

3.3 Apparent solubility analysis

The results of solubility study of Mlx and Mlx-PL complex in various organic solvents and in water showed increased solubility. The Mlx was poorly soluble in water but the Mlx-PL complex shows enhanced solubility and dissolution behaviour. There were few fold increased in solubility of Mlx was observed after preparation of Mlx-PL complex.

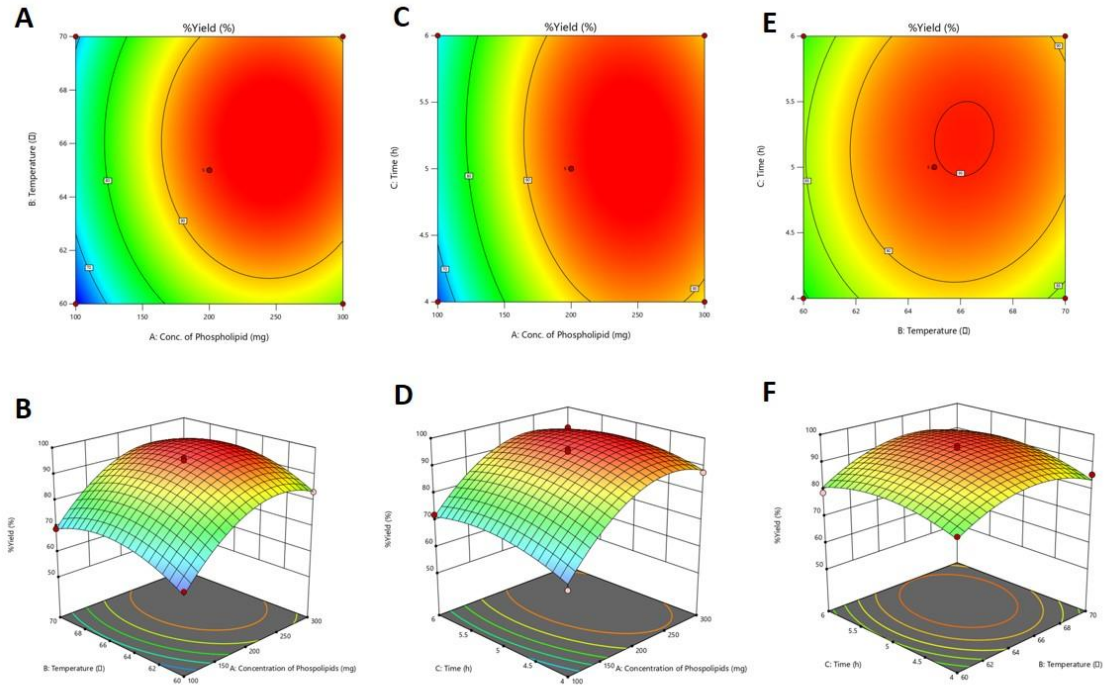

Figure 1: Contour and 3D surface plots of phospholipid concentration and reaction time against percentage yield (A, B), phospholipid concentration and reaction temperature against percentage yield of Mlx-PL complex (C, D), and reaction temperature and reaction time against percentage yield (Y) of Mlx-PL complex (E, F), respectively.

3.4 Physicochemical characterization

3.4.1 Particle Size and Zeta Potential

For the purpose of researching the material's hydrodynamic diameter, particle size measurement is a crucial variable. The determination of particle size and size distribution can be fundamentally researched because the particle size also influences the material's solubility. Prior art claims that particle size also plays a significant impact in material transport across membranes. It might also be in charge of the increased kinetic solubility and bioavailability of poorly soluble drugs or bioactives [15]. Previous research demonstrated that particles with a size between 200 and 400 nm were much more bioavailable than the original substance or material's micro-sized particles [23, 24].The Mlx-PL complex's particle size was determined by zetasizer measurement to be about 122.4 nm (see Figure 2A). However, it was discovered that the Mlx-PL complex's zeta potential value was −35.8 mV, which is lower than 30 mV (see Figure 2B). It demonstrated the Mlx-PL complex's notable physical stability [25, 26]. As the surface charge increases the zeta potential also increases [27].

3.4.2 Thermal analysis

DSC can be used to examine the thermal behaviour of chemical substances and materials. Examining the physical interactions between the various medicinal ingredients is a well-known technique. Additionally, this DSC can test for degradation, compatibility, and stability. Thermal study of Mlx and Mlx-PL complex showed a difference in melting point, indicating that Mlx was successfully trapped in phospholipid complex. This was further reinforced by the absence of phospholipon 90H's distinctive peak. Phospholipon® 90H showed a peak at a lesser intensity at 83.82 °C and a sharp peak at 104.63 °C in a study of its thermal behaviour. These peaks show where phospholipon® 90H melts and changes phases. The physical mixing of Mlx and Phospholipon 90®H, as well as the findings of the thermal analysis, provided evidence of the drug's compatibility with excipients.

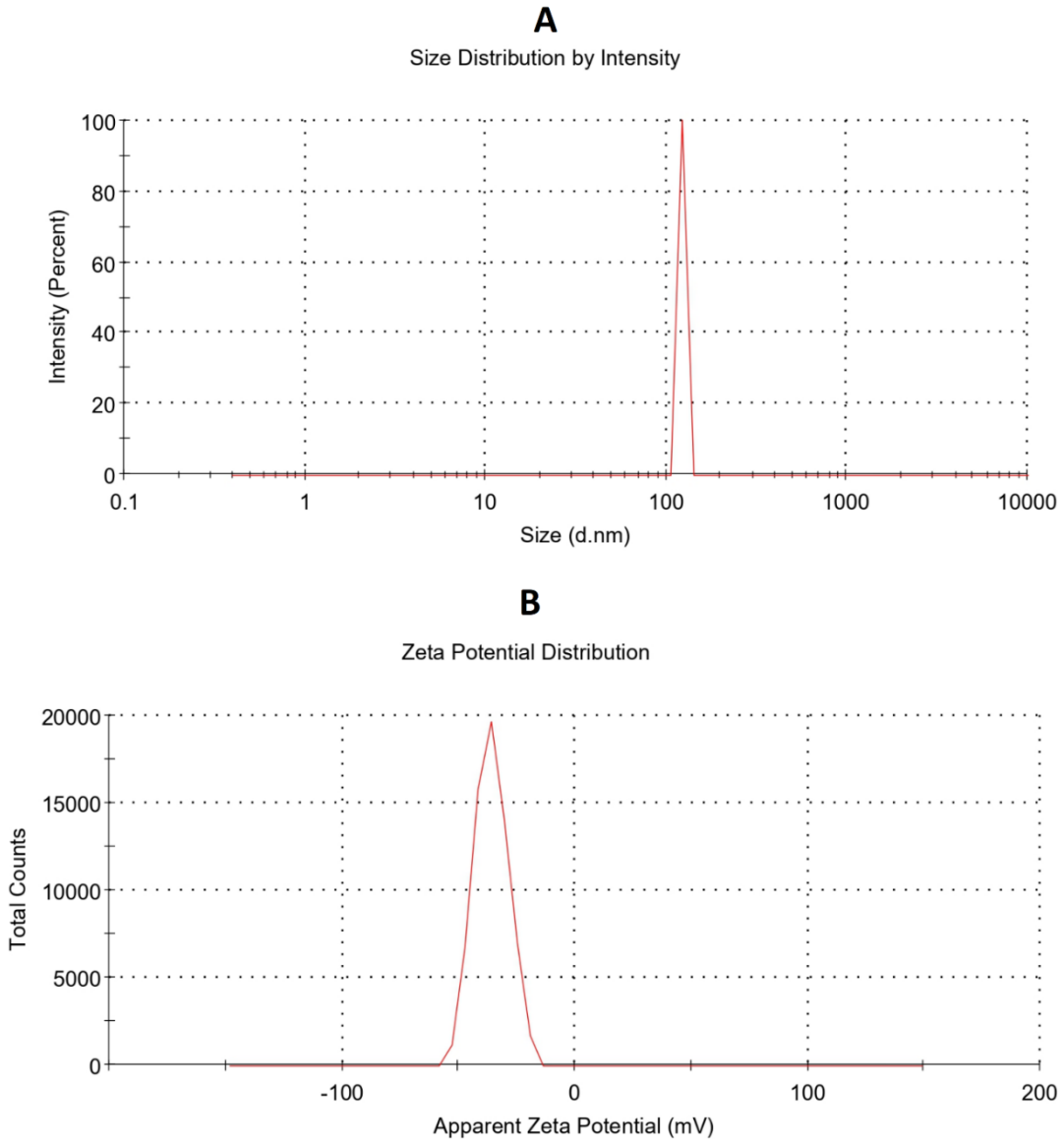

Figure 2: Particle size measurements of optimized Mlx-PL complex made by solvent

evaporation method shows a hydrodynamic diameter of 122.4 nm (red peak) (A) and ζ -potential measurement of Mlx-PLcomplex of −35.8 mV (B).

3.4.3 FTIR spectroscopy

The physical mixing of Mlx and Phospholipon® 90H is shown in Figure 3 along with the FTIR spectra of Mlx, Phospholipon® 90H, the Mlx-PL complex, and Mlx. The spectrum of Mlx displays the typical peaks for Mlx at 3288.63 (O-H), the NH_2 scissoring vibrations band is at or near 1619 cm^1, the secondary amine stretching band is at or near 1550.04 and 1530.36 cm^1, the C N stretching band is at or near 1550.04 and 1530.36 cm^1, and the S-O stretching band is at or near 1346.73, 1265.88, and 1183 cm^1(see Figure 3A). Literature reported the signals for Phospholipon® 90H at 2917.46 and 2849.95 that show the C-H stretching of long fatty acid chains and signals for C=O stretching, P=O stretching, P-O-C stretching, and N+ (CH2)3, respectively [28, 29].

The characteristic peaks of each component in PM can be seen in the spectra of PM from Mlx and Phospholipon® 90H at 3285.45, 2881.95, 1616.88, 1283.74, and 1061.17, respectively (see Figure 3B). This demonstrated Mlx and Phospholipon® 90H's compatibility, which eventually leads in the absence of any physicochemical interaction between them. The peak locations for the Mlx-PL complex are 2917.85, 1736.06, 1293.79, and 1112.16 cm^{-1}as shown in figure 3C. The occurrence of peaks with comparable stretching frequencies and insignificant shifts from 3285.45, 1616.88, and 1061.17 cm^{-1} revealed the Mlx and Phospholipon® 90H's poor intermolecular interaction. The overall FTIR result was interpreted as the lack of interaction between the components employed to prepare the Mlx-PL complex.

3.4.4 Powder X-ray diffraction (P-XRD)

Powder X-ray diffraction is a method for examining the shape of individual particles; in this case, the diffractogram showed whether the substance was crystalline or amorphous. Any material's crystallinity is a crucial characteristic because it directly affects how soluble it is. The shape of Mlx, Phospholipon® 90H, the physical combination of Mlx and Phospholipon® 90H, and the Mlx-PL complex as illustrated in figure 4 were all demonstrated by P-XRD in this case. The crystalline character of Mlx was shown by the sharp and powerful peak at 2θ=23.35° with about 3763 Lin (counts) in the diffractogram shown in Figure 4A. The peak at 2θ=21.34° in Figure 4B is a little bit broader, has a higher intensity, and has around 5051 Lin (Counts) of reduced crystallinity for phospholipon 90 H. The XRD pattern for the physical mixture of Mlx and Phospholipon 90H is shown in Figure 4C. It represents a strong

peak at 2θ=25.80° with a greater intensity and around 1907 Lin (Counts). Figure 4D contrasts this sharp peak at 2θ=25.81° and roughly 2775 Lin (Counts) with another peak at 2θ=39.86° (1221 Lin counts), which is a completely new peak that isn't seen in any of the diffractograms. Therefore, the Mlx-PL complex's diffractogram's existence of a newer peak and lack of the characteristic peaks of Mlx and Phospholipon 90H represent the complex's successful formation with a novel pattern of crystallinity. All the results obtained during P-XRD were resembles to previously reported in literature [30, 31].

3.4.5 SEM analysis

SEM was used to study the surface morphology of the Mlx-PL complex, and structural traits were identified by looking at SEM pictures, as shown in figure 5A. This image depicts the Mlx-PL complex's rough surface. The complex's porous surface allowed a solvent or other media to enter and start the solubilization process.

3.5 Entrapment efficiency

The %EE of optimized formulation of Mlx-PL complex was found to be 91.77 ± 1%.

3.6 *In vitro* drug release study

The drug release study of Mlx from the Mlx-PL complex and Mlx suspension was carried out in buffer pH 7.4. The results obtained in this study demonstrated the 94.85±3.0 % release of Mlx was observed after 72 h and initial burst release of Mlx was found to be 26.26% in first two hours. However Mlx suspension releases about 94% drug within 6 h as shown in figure 5B. Hence from these observations we can concluded the controlled release of drug for longer period of time. This could be happened due to the formation of phospholipid complex in which Mlx was encapsulated in the internal core of complex.

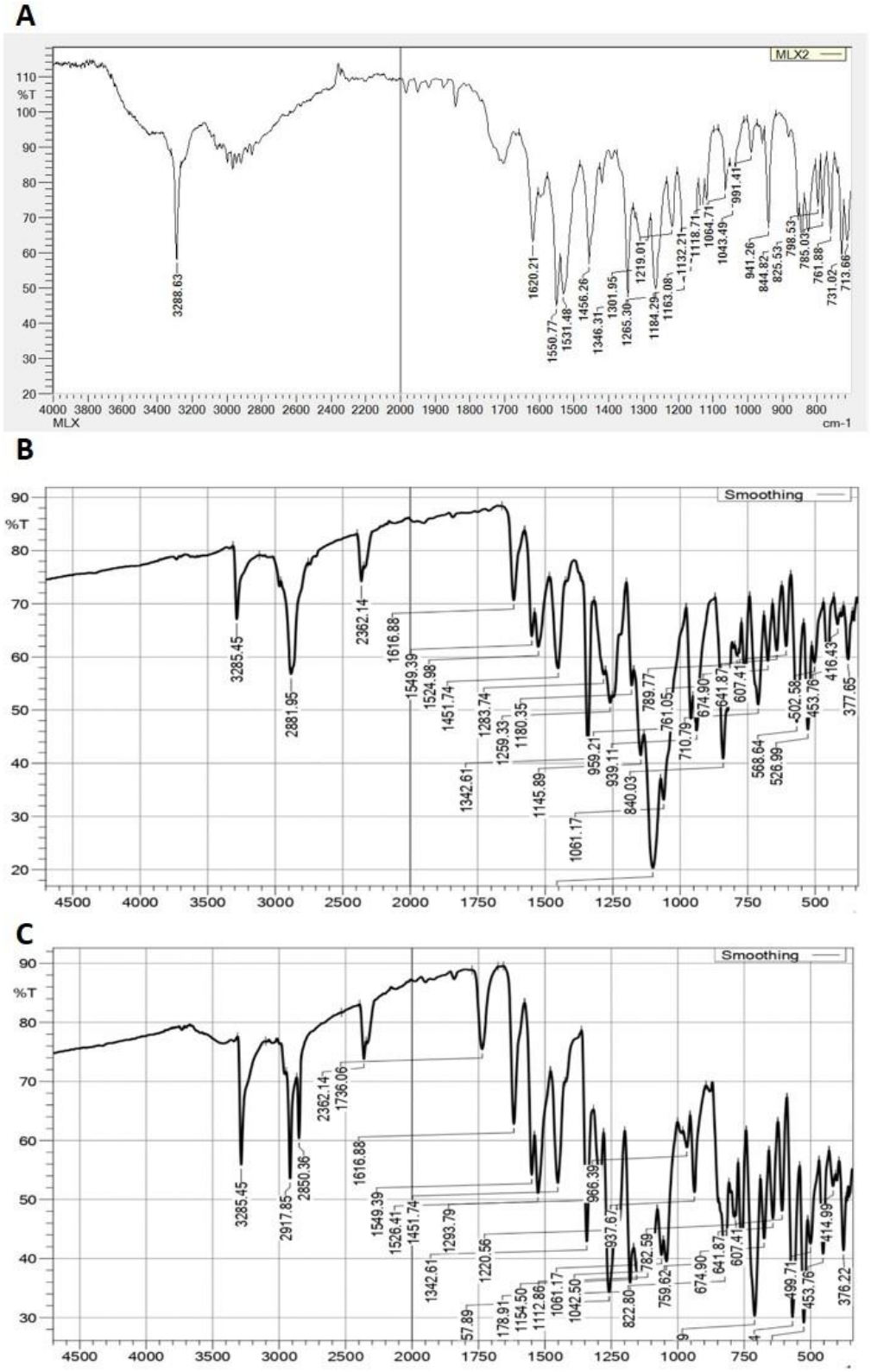

Figure 3:FTIR Spectrum of Mlx (A), Physical Mixture of Mlx and Phospholipon 90® H (B), Mlx-PL complex (C).

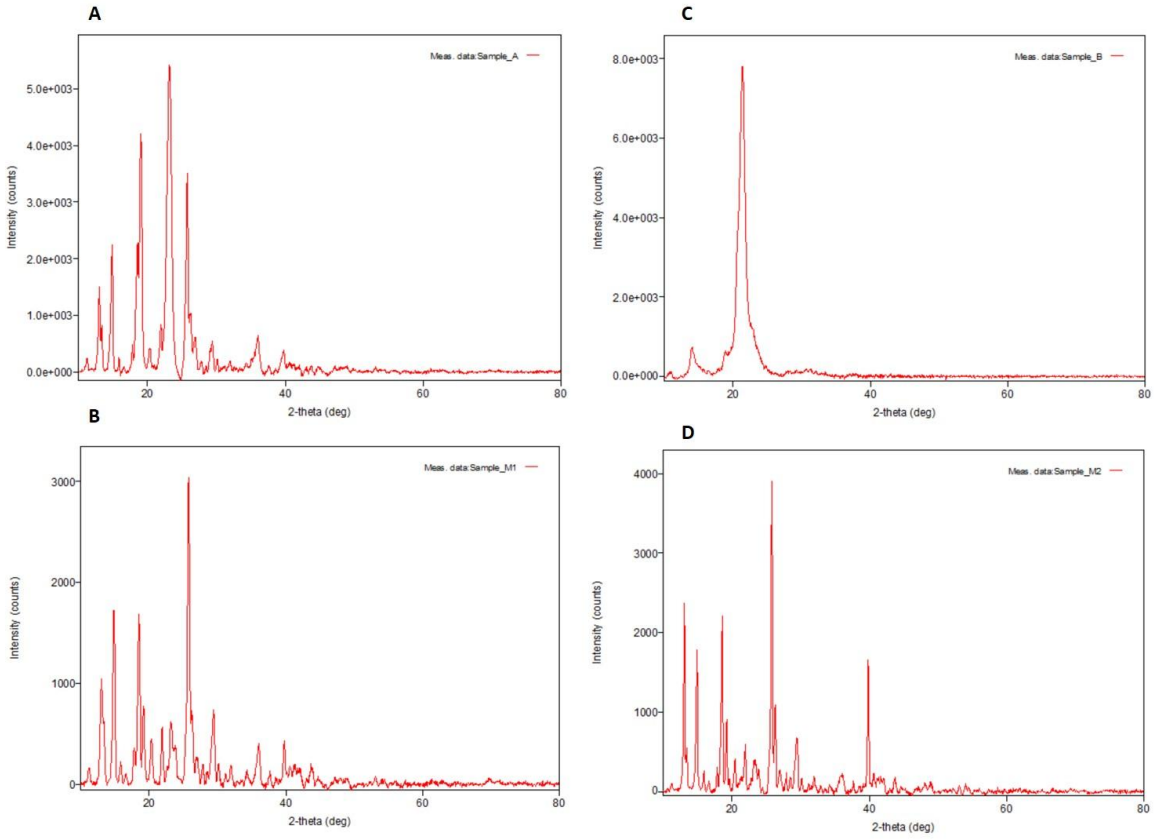

Figure 4: The X-ray diffractogram of pure A)Mlx, B) Phospholipon® 90H, C) physical mixture of Mlx and Phospholipon® 90H and D) the Mlx-PL complex showing crystalline nature at 2θ=23.35°, 2θ=21.34°, 2θ=25.80°, 2θ=25.81° and 2θ =39.86°, respectively.

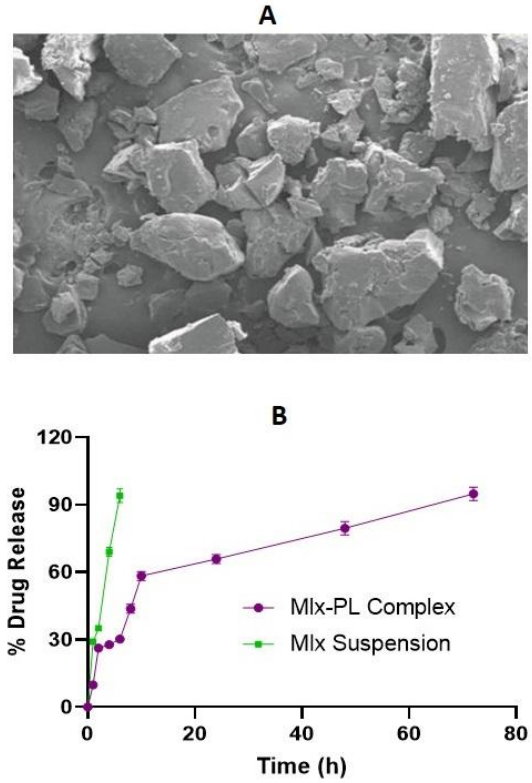

Figure 5:(A) The scanning electron microscopic images depicts rough surface of the Mlx-PL complex, (B) % drug release from Mlx suspension and Mlx-PL complex showing controlled release of drug upto 72h.

3.7 *In vitro* cytotoxicity

Figure 6 depicts the cytotoxicity of pure Mlx and Mlx-PL combination on MCF-7 cells. More than 90% of cells thrive and multiply relative to controls PBS and DMSO, which implies that these substances are not harmful (Figure 6A). According to the data presented in figure 6B, pure Mlx dissolved in DMSO at doses of 0.01, 0.1, 1, 10, 100, and 1,000 µg/mL significantly inhibited MCF-7 cells less than Mlx-PL complex. After 72 h, the Mlx-PL combination and pure Mlx in DMSO were found to have IC50 (50% inhibition) values of 4.3 and 6.2 M, respectively. The MTT test was used to evaluate the anti-proliferative effect of Mlx-PL complex combination on MCF-7 at varied doses. Following treatment, the MCF-7 cells displayed no toxicity to DMSO or phosphate buffered saline solution. But when the concentration of Mlx-PL complex is raised, both Mlx in-DMSO and Mlx-PL complex exhibit considerable toxicity with increased relative inhibition. The results of the cell toxicity investigation showed that the sustained release of Mlx after the creation of the phospholipid complex (Mlx-PL) led to a greater relative inhibition (%) of MCF-7 cells for the Mlx-PL complex than for pure Mlx dissolved in DMSO.

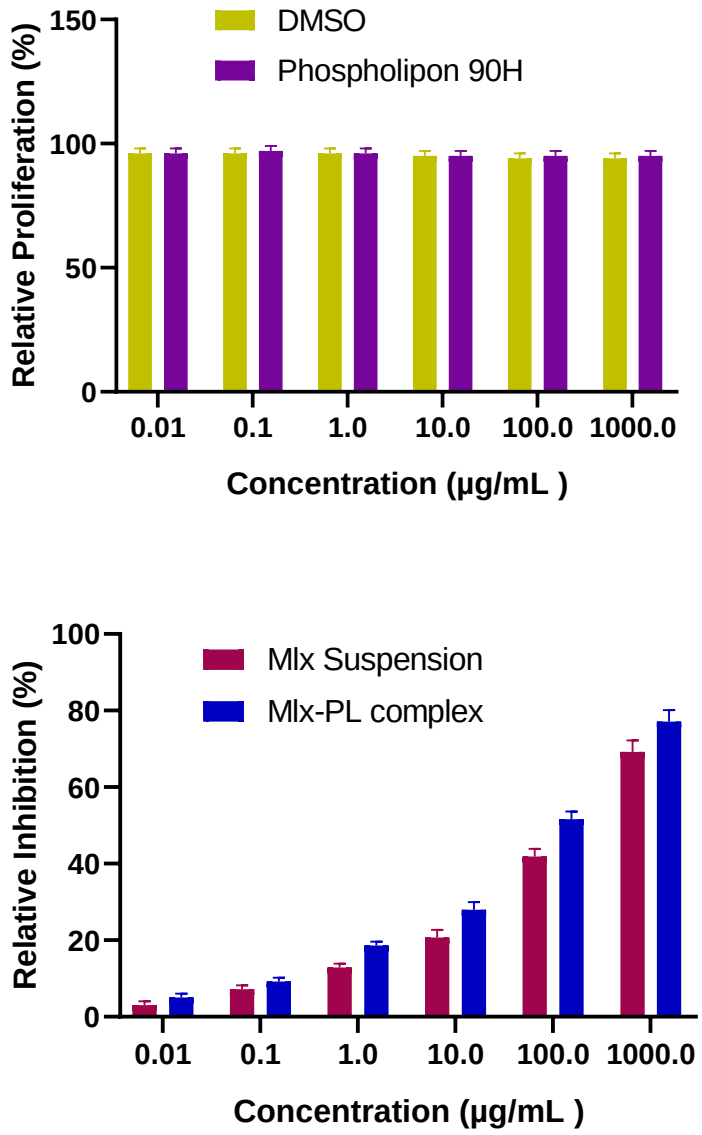

Figure 6: Effects of Mlx-PL complex, Mlxsuspension, and DMSO on MCF-7 human breast cancer cells. Human breast adenocarcinoma cells (MCF-7) were used to study the *in vitro* cytotoxicity of Mlx-PL complex and Mlxsuspension using the MTT assay. Cells were then analysed after 72 hours on SpectraMax M2. The bars depict mean and SD (n = 3). The percentages of relative proliferation (A) and inhibition (B) are used to express the results.

4. Conclusion

The Mlx-PL complex was synthesized by solvent evaporation method and the formula containing Mlx and Phospholipon® 90H in the ratio of 1:2 was optimized using BBD design. The prepared Mlx-PL complex shows more solubility than the pure Mlx in water hence the solubility of the poorly water soluble drug could be increased by phospholipid complex formation. The optimized Mlx-PL complex demonstrated the lower particle size and excellent

colloidal stability.*In vitro*cytotoxicity study revealed higher efficiency of Mlx-PL complex in MCF-7 cell lines than the pure Mlx suspension. The overall results of this study proved the excellent potential of phospholipid complex for solubility enhancement and improved efficacy of the anticancer drugs which belongs to BCS class II.

Conflict of interest

Authors declare no conflict of interest.

Contribution

VAB and PSK design the study protocol. VAB executed the project and performed the experiments and analysis. VAB, PSK were involved in data interpretation, drafting and reviewing of manuscript for final submission.

References

1. Rarokar N, Gurav S, Khedekar P. Meloxicam encapsulated nanostructured colloidal self- assembly for evaluating antitumor and anti- inflammatory efficacy in 3D printed scaffolds. Journal of Biomedical Materials Research Part A. 2021 Aug;109(8):1441-56.

2. Bolourchian N, Nili M, Shahhosseini S, Nokhodchi A, Foroutan SM. Crystallization of meloxicam in the presence of hydrophilic additives to tailor its physicochemical and pharmaceutical properties. Journal of Drug Delivery Science and Technology. 2021 Dec 1;66:102926.

3. Saoji SD, Raut NA, Dhore PW, Borkar CD, Popielarczyk M, Dave VS. Preparation and evaluation of phospholipid-based complex of standardized centella extract (SCE) for the enhanced delivery of phytoconstituents. The AAPS journal. 2016 Jan;18:102-14.

4. Saoji SD, Dave VS, Dhore PW, Bobde YS, Mack C, Gupta D, Raut NA. The role of phospholipid as a solubility-and permeability-enhancing excipient for the improved delivery of the bioactive phytoconstituents of Bacopa monnieri. European Journal of Pharmaceutical Sciences. 2017 Oct 15;108:23-35.

5. Telange DR, Patil AT, Pethe AM, Fegade H, Anand S, Dave VS. Formulation and characterization of an apigenin-phospholipid phytosome (APLC) for improved solubility, in vivo bioavailability, and antioxidant potential. European Journal of Pharmaceutical Sciences. 2017 Oct 15;108:36-49.

6. Telange DR, Nirgulkar SB, Umekar MJ, Patil AT, Pethe AM, Bali NR. Enhanced transdermal permeation and anti-inflammatory potential of phospholipids complex-loaded matrix film of umbelliferone: Formulation development, physico-chemical and functional characterization. Eur J Pharm Sci. 2019 Apr 1;131:23-38. doi: 10.1016/j.ejps.2019.02.006. Epub 2019 Feb 5. PMID: 30735820.

7. Zhang Z, Lin Y, Liu F. Preparation and characterization of CdS/ZnS core-shell nanoparticles. Journal of Dispersion Science and Technology. 2020 Apr 15;41(5):725-32.

8. Chan JM, Zhang L, Yuet KP, Liao G, Rhee JW, Langer R, Farokhzad OC. PLGA–lecithin–PEG core–shell nanoparticles for controlled drug delivery. Biomaterials. 2009 Mar 1;30(8):1627-34.

9. Fricker G, Kromp T, Wendel A, Blume A, Zirkel J, Rebmann H, Setzer C, Quinkert RO, Martin F, Müller-Goymann C. Phospholipids and lipid-based formulations in oral drug delivery. Pharmaceutical research. 2010 Aug;27(8):1469-86.

10. Hou Z, Li Y, Huang Y, Zhou C, Lin J, Wang Y, Cui F, Zhou S, Jia M, Ye S, Zhang Q. Phytosomes loaded with mitomycin C–soybean phosphatidylcholine complex developed for drug delivery. Molecular pharmaceutics. 2013 Jan 7;10(1):90-101.

11. Rajbhar K, Karodadeo GR, Kumar V, Barethiya V, Lahane A, Kale S, Thakre V, Dixit G, Kohale N, Hiradeve S, Rarokar NR. Comparative assessment of solubility enhancement of itroconazole by solid dispersion and co-crystallization technique: Investigation of simultaneous effect of media composition on drug dissolution. InAnnalesPharmaceutiquesFrançaises 2023 May 12. Elsevier Masson.

12. Preethi V, Ramesh ST, Gandhimathi R, Nidheesh PV. Optimization of batch electrocoagulation process using Box-Behnken experimental design for the treatment of crude vegetable oil refinery wastewater. Journal of Dispersion Science and Technology. 2019 Apr 15.

13. Rarokar NR, Khedekar PB, Bharne AP, Umekar MJ. Development of self-assembled nanocarriers to enhance antitumor efficacy of docetaxeltrihydrate in MDA-MB-231 cell line. International journal of biological macromolecules. 2019 Mar 15;125:1056-68.

14. Saoji SD, Rarokar NR, Dhore PW, Dube SO, Gurav NS, Gurav SS, Raut NA. Phospholipid based colloidal nanocarriers for enhanced solubility and therapeutic efficacy of withanolides. Journal of Drug Delivery Science and Technology. 2022 Apr 1;70:103251.

15. Rarokar NR, Saoji SD, Raut NA, Taksande JB, Khedekar PB, Dave VS. Nanostructured cubosomes in a thermoresponsive depot system: an alternative approach for the controlled delivery of docetaxel. AAPS pharmscitech. 2016 Apr;17:436-45.

16. Rarokar NR, Telange DR, Kalsait RP, Khedekar PB. Solubility enhancement of extract of Lagenariasiceraria by development of Phospholipon® 90 H modulated phospholipid complex employing Box-Behnken design. InAnnalesPharmaceutiquesFrançaises 2022 Nov 11. Elsevier Masson.doi:10.1016/j.pharma.2022.11.007

17. Rarokar NR, Menghani SS, Kerzare DR, Khedekar PB, Bharne AP, Alamri AS, et al.

Preparation of Terbinafin-Encapsulated Solid Lipid Nanoparticles Containing Antifungal Carbopol® Hydrogel with Improved Efficacy: In Vitro, Ex Vivo and In Vivo Study. Pharmaceutics [Internet] 2022;14(7):1393.

18. Rarokar N, Agrawal R, Yadav S, Khedekar P, Ravikumar C, Telange D, Gurav S. Pteroyl-γ-l-glutamate/Pluronic® F68 modified polymeric micelles loaded with docetaxel for targeted delivery and reduced toxicity. Journal of Molecular Liquids. 2023 Jan 1;369:120842.

19. Rodrigues K, Nadaf S, Rarokar N, Gurav N, Jagtap P, Mali P, Ayyanar M, Kalaskar M, Gurav S. QBD approach for the development of hesperetin loaded colloidal nanosponges for sustained delivery: In-vitro, ex-vivo, and in-vivo assessment. OpenNano. 2022 Jul 1;7:100045.

20. V. Paruchuri, A. Nguyen, J. Miller, Zeta-potentials of self-assembled surface micelles of ionic surfactants adsorbed at hydrophobic graphite surfaces, Colloids and Surfaces A: Physicochemical and Engineering Aspects 250(1-3) (2004) 519-26.

21. X. Zeng, W. Tao, L. Mei, L. Huang, C. Tan, S. Feng, Cholic acid-functionalized nanoparticles of star-shaped PLGA-vitamin E TPGS copolymer for docetaxel delivery to cervical cancer, Biomaterials 34(25) (2013) 6058-67.

22. S. Feng, H. Zhang, S. Xu, C. Zhi, Nakanishi H, Gao XD. Folate-conjugated, mesoporous silica functionalized boron nitride nanospheres for targeted delivery of doxorubicin, Materials Science and Engineering: C 96 (2019) 552-60.

23. Wang H, Li Q, Reyes S, Zhang J, Xie L, Melendez V, Hickman M, Kozar MP. Formulation and particle size reduction improve bioavailability of poorly water-soluble compounds with antimalarial activity. Malaria Research and Treatment. 2013;2013.

24. Freitas C, Müller RH. Effect of light and temperature on zeta potential and physical stability in solid lipid nanoparticle (SLN™) dispersions. International journal of pharmaceutics. 1998 Jun 15;168(2):221-9.

25. Elnakat H. Distribution, functionality and gene regulation of folate receptor isoforms: implications in targeted therapy. Advanced drug delivery reviews. 2004 Apr 29;56(8):1067-84.

26. O'Shannessy DJ, Somers EB, Palmer LM, Thiel RP, Oberoi P, Heath R, Marcucci L. Serum folate receptor alpha, mesothelin and megakaryocyte potentiating factor in ovarian cancer: association to disease stage and grade and comparison to CA125 and HE4. Journal of ovarian research. 2013 Dec;6(1):1-6.

27. Allard JE, Risinger JI, Morrison C, Young G, Rose GS, Fowler J, Berchuck A, Maxwell GL. Overexpression of folate binding protein is associated with shortened progression-free survival in uterine adenocarcinomas. Gynecologic oncology. 2007 Oct

1;107(1):52-7.

28. Yin H, Lin Y, Huang J. Microstructures and rheological dynamics of viscoelastic solutions in a catanionic surfactant system. Journal of Colloid and Interface Science. 2009 Oct 1;338(1):177-83.

29. Yin H, Lin Y, Huang J. Microstructures and rheological dynamics of viscoelastic solutions in a catanionic surfactant system. Journal of Colloid and Interface Science. 2009 Oct 1;338(1):177-83.

30. Pandya R, Mehta T, Gohel M. Amalgamation of solid dispersion and adsorption technique: A case study of ritonavir. Journal of Thermal Analysis and Calorimetry. 2015 Apr;120:699-709.

31. Yang JH, Zhang L, Li JS, Chen LH, Zheng Q, Chen T, Chen ZP, Fu TM, Di LQ. Enhanced oral bioavailability and prophylactic effects on oxidative stress and hepatic damage of an oil solution containing a rosmarinic acid–phospholipid complex. Journal of functional foods. 2015 Dec 1;19:63-73.